ASEAN
Journal of Scientific and Technological Reports
Online ISSN:2773-8752

Research article

Approach for Boosting the Drying Chamber's Temperature by Pulse Copper Pipes to Conduct Heat

Kitti Korbuakaew[1], and Prasit Phoosomma[2*]

[1] Faculty of Science and Technology, Dhonburi Rajabhat University, Thonburi, Bangkok, 10600, Thailand
[2] Faculty of Science and Technology, Dhonburi Rajabhat University, Thonburi, Bangkok, 10600, Thailand
* Correspondence: prasit.p@dru.ac.th

Citation:
Approach for boosting the drying chamber's temperature by pulse copper pipes to conduct heat. *ASEAN J. Sci. Tech. Report.* **2025**, *28*(3), e254983. https://doi.org/10.55164/ajstr.v28i3.254983

Article history:
Received: July 11, 2024
Revised: April 25, 2025
Accepted: May 12, 2025
Available online: May 31, 2025

Abstract: This research addresses a critical challenge in solar food drying: maintaining effective drying performance during low solar radiation intensity periods. We present an innovative hybrid drying system that combines thermal energy from direct solar radiation with supplementary heat provided by hot water circulating through strategically positioned copper pipes. The pulse copper pipe configuration conducts additional heat within the drying chamber, significantly enhancing thermal performance when outdoor temperatures drop or sunlight is limited. Experimental results demonstrate that this hybrid approach increases the temperature inside the drying chamber and extends drying periods by at least 10 minutes under low heat radiation conditions. Most notably, the combination of air drying with infrared radiation and hot water circulation yielded a 4.25% improvement in thermal efficiency compared to conventional methods. This approach represents a promising advancement in sustainable food preservation technology, particularly for regions with variable weather conditions.

Keywords: Conduct heat; drying chamber; pulse copper pipes; solar drying technology; hybrid thermal systems

1. Introduction

Solar radiation energy has emerged as a critical resource in contemporary sustainable technologies. While the sun has served as humanity's natural method for food drying throughout history, technological advancement has led to the development of sophisticated solar dryers that enhance this process [1,2]. Recent experimental validation has confirmed the heat efficiency of parabolic trough solar air heaters (PTSAH) utilizing U-shaped copper and aluminum heat exchangers, both with and without fins [3-4]. These systems have demonstrated considerable success in directly drying various agricultural products, including plantains, bananas, mangoes, and cassava through natural heat convection mechanisms [5-6].Innovation in this field continues with hybrid solar systems that harness the Joule effect generated by parallel-connected photovoltaic modules to efficiently dry sliced potatoes and similar food products [7-9]. Despite the availability of diverse drying technologies, comparing their effectiveness remains challenging due to variations in protective mechanisms and product-specific drying requirements. The implementation of standardized performance metrics could significantly streamline evaluation procedures.

The concept of necessary drying capability has driven improvements in solar dryers, substantially enhancing air drying capacity. Research has explored

using duck pods to increase moisture content in experimental settings, with integrated solar dryers proving particularly accessible and efficient [11-13]. These systems offer simple, expedient equipment for processing duck pods, allowing for complete same-day processing even without predetermined drying rates [12].Significant advancements in installation systems have increased annual solar energy utilization from 28.9% to 50.5%. Premium installation configurations employ adaptation tanks for solar hot water storage, connecting them in series with compact heating tanks to achieve annual performance ratings up to 50.5% [13-14]. This configuration allows larger tanks to operate at lower average temperatures while smaller, well-insulated tanks maintain higher temperatures, effectively reducing heat loss and enhancing solar engagement. Independent conventional heating systems can account for 52% of total energy needs in comparable storage conditions, with storage and reference conditions being primary factors. These parallel systems offer potentially lower investment costs while maintaining comparable performance metrics.

Heat pump-equipped solar collectors have gained widespread adoption for capturing solar energy in unfavorable sunlight conditions [15-17]. Solar water heating systems (SWHS) efficiency depends significantly on refrigerant selection, suggesting the need for developing superior refrigerants to enhance future performance [18-19]. Economic feasibility assessment requires consideration of multiple factors, while achieving consumer preference necessitates a comprehensive analysis of flow dynamics and heat transfer behaviors in solar collectors [24-26].The development of solar-powered food processing drying cabinets [10] utilizing solar-heated pipes has advanced the field further. These systems account for energy efficiency during the drying process and final product quality. Research confirms that moisture reduction correlates with increased drying time and temperature, with optimal results above 50°C. A significant advantage of these systems is their independence from electrical inputs, offering substantial energy conservation benefits.

Pulsating heat pipes have garnered significant research attention for their thermal performance and efficiency [19-23]. These innovative heat transfer devices provide enhanced thermal conductivity and have been applied across applications ranging from solar to cryogenic temperatures [21, 29]. Their integration into solar drying systems represents a promising frontier in thermal efficiency improvement.This research provides practical guidelines for food drying under suboptimal light conditions, including rainy periods, darkness, or limited sunlight exposure, expanding solar drying technologies' versatility and application scope in diverse environmental contexts. By incorporating pulse copper pipes to conduct heat within the drying chamber, we address a critical challenge in maintaining drying efficiency during periods of low solar radiation, contributing to more reliable and energy-efficient food preservation methods [27-28].

2. Materials and Methods

2.1 General (original model drying cabinet)

Farmers have traditionally relied on traditional sun-drying techniques for food preservation, as illustrated in Figure 1. This approach gained widespread adoption primarily due to economic considerations, as it significantly reduced household expenditures by eliminating the need for technological investments. The conventional methodology typically involved direct exposure of agricultural products to solar radiation in open environments. However, this traditional approach presents several substantial challenges, including contamination from environmental particulates (dust and PM 2.5) and vulnerability to insect vectors that potentially transmit pathogenic microorganisms. Researchers have developed enclosed solar drying systems to address these limitations while maintaining the benefits of solar energy utilization. These improved systems, exemplified by the solar oven configuration depicted in Figure 2, provide a protected environment that maintains drying efficiency while substantially reducing contamination risks.

Figure 1. Historically, through sun-drying

Figure 2. Original model drying cabinet

2.2 Synthesis (add to pulsed copper heating pipes)

Despite the improvements over traditional sun-drying methods, conventional solar dryers still exhibit significant operational limitations. A primary constraint is their thermal inefficiency during periods of reduced solar radiation, such as cloudy days or evening hours, when the temperature within the drying chamber decreases substantially below optimal levels. This temperature reduction compromises the drying process and extends processing time, reducing productivity and potentially affecting product quality. To address these limitations, we have developed an enhanced hybrid drying system integrating infrared radiation with controlled hot water circulation through pulsed copper heating pipes. This innovative design enables rapid thermal response, achieving significant temperature elevation within the drying chamber in approximately one minute. The system operates through convective heat transfer, storing hot water in a dedicated reservoir. Thermal energy is efficiently conducted and radiated throughout the drying chamber via strategically positioned pulsed copper heating pipes, as illustrated in Figure 3. The complete assembly of the new solar drying cabinet with the integrated pulsing heat pipe configuration is presented in Figure 4. This hybrid approach ensures consistent drying conditions even during unfavorable ambient conditions, extending operational hours and enhancing overall system reliability and efficiency.

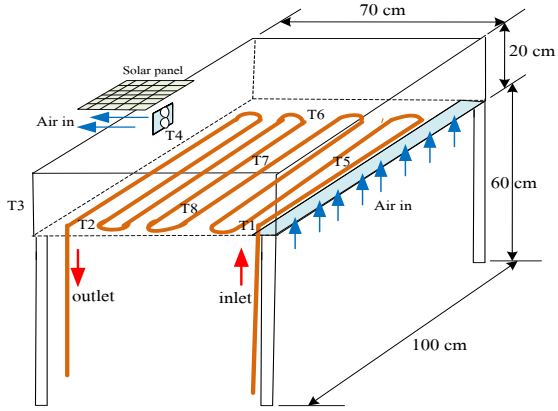

Figure 3. The pulse copper heat pipe is positioned within the drying chamber, and the temperature measurement site is displayed.

Figure 4. New solar drying cabinet and pulsing heat pipes' placement

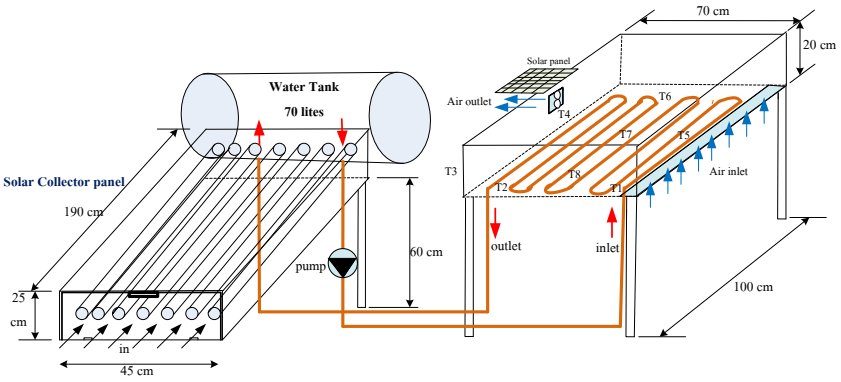

Figure 5. Infrared thermal energy drying system design

2.3 Experimental Setup and System Specifications

The experimental apparatus consists of three primary components: a solar collector, a water storage tank, and the drying chamber equipped with pulsed copper heating pipes. The solar collector (dimensions: 45 cm × 190 cm) employs a flat-plate design with a selective absorber coating to maximize thermal energy capture. The collector was oriented facing south at an inclination angle of 15° to optimize solar radiation collection at the experimental location (latitude 7.6°N, longitude 100.1°E). The water storage tank has a capacity of 70 liters and is constructed from stainless steel with 25 mm polyurethane foam insulation (thermal conductivity: 0.023 W/m·K) to minimize heat losses. A 45W solar-powered circulation pump (flow rate: 2.5 L/min) transfers heated water from the collector to the storage tank and subsequently to the pulsed copper pipe network within the drying chamber. The drying chamber measures 100 cm × 70 cm × 60 cm and is fabricated from an aluminum frame with 4 mm tempered glass on the top surface. The chamber is insulated with 20 mm polyurethane foam on all non-transparent surfaces. The pulsed copper pipe network consists of 12 mm diameter copper pipes (thermal conductivity: 401 W/m·K) arranged in a serpentine configuration with a total pipe length of 7.2 meters. The pipes are spaced 10 cm apart to ensure uniform heat distribution throughout the drying chamber. The system incorporates eight temperature measurement points (T_1-T_8) strategically positioned as shown in Figure 3 to monitor temperature distribution and gradients within the drying chamber.

2.4 Instrumentation and Data Acquisition

Temperature measurements were conducted using calibrated T-type thermocouples (measurement range: -50°C to 150°C, accuracy: ±0.5°C) connected to a data acquisition system (Agilent 34972A) with a scanning rate of 30 seconds. Solar radiation intensity was measured using a calibrated pyranometer (Kipp & Zonen CMP6, sensitivity: 5-20 μV/W/m², spectral range: 285-2800 nm) mounted on a horizontal surface adjacent to the solar collector. Ambient conditions, including temperature, relative humidity, and wind speed, were monitored using an automated weather station (Davis Vantage Pro2) with recording intervals of 5

minutes. The moisture content of food samples was determined using oven drying according to AOAC standards (Method 934.01). Samples were weighed using an analytical balance with 0.001 g precision at predetermined time intervals throughout the drying process to establish moisture reduction curves.

2.5 Experimental Procedure

The experimental trials were conducted over three months (February-April 2024) to evaluate system performance under varying weather conditions. Each experimental run was initiated at 08:00 and continued until 16:00 to capture the full diurnal cycle of solar radiation. Before each experiment, the water tank was filled with fresh water and allowed to preheat for 60 minutes. Three operational modes were evaluated to compare performance for direct sun drying (DR) - traditional open-air drying, solar drying cabinet without supplementary heating (SR), and solar drying cabinet with pulsed copper pipe heating at three temperature setpoints: 50°C, 60°C, and 70°C (SR+W50, SR+W60, SR+W70). For each operational mode, identical food samples (100 g, initial moisture content 80-85% w.b.) were prepared and distributed evenly on drying trays. Temperature readings and sample weights were recorded at 30-minute intervals throughout the drying process.

2.6 Performance Evaluation Metrics

The thermal efficiency of the solar collector and overall system was evaluated using established heat transfer equations described in Section 3. Specifically, the collector efficiency was calculated using Equation (3), while dryer efficiency was determined using Equation (4). Different operational modes were compared based on drying rate, specific energy consumption, and final product quality.Statistical analysis was performed using SPSS software (version 26.0) with a significance level of $p < 0.05$. All experiments were conducted in triplicate, and results are presented as mean values with standard deviations to ensure reproducibility and statistical validity.

3. Results and Discussion

The performance assessment of solar water heating systems requires consideration of three fundamental thermal load components. The primary component involves heating water to the desired temperature, necessitating a specific rate of sensible heat addition. This rate depends on several factors, including the mass flow rate of water, initial supply temperature, and target delivery temperature. The subsequent sections analyze the thermal efficiency parameters and solar radiation characteristics influencing the system's performance.

3.1 Thermal efficiency analysis

The useful thermal energy (Q_u) obtained from air flowing through the solar collector can be calculated using the energy balance equation [6,15]:

$$Qu = mCp\,(Td - Ts) \quad (1)$$

Where Qu represents the useful thermal energy gained (W), $\dot{m}$ denotes the mass flow rate of the working fluid (kg/s), Cp is the specific heat capacity of the fluid (J/kg·K), Td indicates the delivery temperature (°C), and Ts corresponds to the supply temperature (°C). This fundamental equation enables quantitative assessment of the thermal energy transfer within the system and provides a basis for determining operational efficiency under varying conditions.

3.2 Solar radiationcharacteristics

Solar radiation intensity at the outer boundary of Earth's atmosphere averages approximately 1361 W/m², known as the solar constant. This value represents the solar irradiance per unit area on a spherical surface surrounding the Sun at a radius equal to Earth's orbital distance (1 Astronomical Unit). From the Sun's perspective, Earth is a circular disc that consistently receives this radiation flux. The intercepting disc has an

area of πr^2, where r denotes Earth's radius, while the planet's total surface area ($4\pi r^2$) results from its spherical geometry [7]. The daily solar energy received at a specific terrestrial location can be calculated using integration.

$$Q^{day} = -\frac{1}{2}\int_{-\pi}^{\pi} Q dh \tag{2}$$

Where Q^{day} represents the daily solar energy received (J/m²), Q denotes the instantaneous solar radiation intensity (W/m²), and h corresponds to the hour angle (radians). The value of Q becomes positive at sunrise, when the hour angle reaches a specific threshold dependent on the location's latitude and the solar declination angle.

3.3 The thermal efficiency of a solar collector

A solar collector's thermal efficiency (η) represents the ratio between the useful energy extracted from the system and the total solar energy input. Specifically, it quantifies the relationship between the thermal energy utilized to increase the working fluid's temperature and the incident solar radiation energy received by the collector surface. According to established thermal performance principles [4,5,6], this efficiency can be expressed mathematically as:

$$\eta = \frac{\dot{m} \times C_p \times (T_{out} - T_{in})}{A_p \times I_o} \tag{3}$$

Where$\dot{m}$ represents the fluid mass flow rate (kg/s), Cp denotes the specific heat capacity of the fluid (J/kg·K), Tout indicates the fluid temperature at the outlet (°C), Tin corresponds to the fluid temperature at the inlet (°C), Ap refers to the effective aperture area of the collector (m²), and Io designates the incident solar radiation intensity (W/m²). This efficiency parameter provides a critical performance metric for evaluating and comparing various solar collector designs and operational conditions.

3.4 Determination of dryer efficiency

Dryer efficiency quantifies the system's effectiveness in utilizing solar energy for moisture removal. It is the ratio of thermal energy employed in the evaporation process to the total solar energy incident on the dryer surface area. Following established methodologies [21,27,28], the dryer efficiency (η) can be calculated using:

$$\eta = \frac{\dot{m} \times h_{fg}}{A_p \times I_o} \tag{4}$$

Where$\dot{m}$ represents the mass flow rate of moisture removal (kg/s), hfg denotes the latent heat of vaporization for water (kJ/kg), Ap corresponds to the effective collector aperture area (m²), and Io indicates the incident solar radiation intensity (W/m²). This efficiency metric enables a comprehensive assessment of the drying system's performance under various operational conditions and design configurations.

3.5 Infrared combined heat and hot water dryer

The developed hybrid drying system integrates infrared radiation with hot water circulation, offering precise temperature control capabilities. The system permits adjusting the drying chamber temperature to three setpoints: 50 °C, 60 °C, and 70 °C, thereby accommodating various product-specific drying requirements. Supplementary thermal energy can be introduced to the drying chamber by transferring accumulated heat from the water storage reservoir. The innovative copper pipe network design facilitates efficient convective heat transfer throughout the drying chamber, ensuring uniform temperature distribution and optimized drying conditions even during periods of limited solar radiation.

3.6 Experimental results and summary

Comprehensive thermal performance data were collected from the experimental setup to evaluate the system's efficiency and temperature distribution characteristics. Temperature measurements within the drying chamber and solar radiation intensity monitoring provided insights into the system's operational dynamics under real-world conditions. Figure 6 illustrates the integrated dryer system with combined heat sources, demonstrating the physical configuration of the experimental apparatus. When operating with the thermostat set at 60 °C, the system demonstrated significant temperature elevation within the drying chamber. The ambient temperature surrounding the drying oven, recorded by sensor T_3, was 35.14 °C, while the drying chamber maintained an average temperature of 52.16 °C, indicating an effective temperature differential of approximately 17 °C. Detailed temperature measurements revealed spatial variations within the chamber, with readings from individual sensors as follows: T_1 (50.33 °C), T_2 (48.67 °C), T_4 (50.22 °C), T_5 (47.27 °C), T_6 (54.31 °C), T_7 (57.43 °C), and T_8 (57.15 °C). Throughout the experimental period, the system operated under variable weather conditions with an average solar radiation intensity of 538.92 W/m². The comprehensive temperature data collected from the chamber sensors are summarized in Table 1. The temporal evolution of temperature within the drying cabinet is graphically represented in Figure 7, while Figure 9 illustrates the solar radiation intensity fluctuations over the experimental duration. Notably, the test day featured alternating periods of clear and cloudy sky conditions, providing valuable data on system performance under variable solar input scenarios.

Figure 6. Dryer with combined heat and energy

With the thermostat configured at 60 °C, comprehensive thermal measurements were obtained throughout the experimental apparatus. The ambient temperature surrounding the drying system, recorded by sensor T_3, registered at 35.14 °C, establishing the baseline environmental condition. Concurrently, the drying chamber maintained a mean temperature of 52.16 °C, demonstrating a significant thermal enhancement of 17.02 °C above ambient conditions. Spatial temperature distribution analysis revealed notable thermal gradients within the chamber, with temperature values varying across measurement locations: T_1 (50.33 °C), T_2 (48.67 °C), T_4 (50.22 °C), T_5 (47.27 °C), T_6 (54.31 °C), T_7 (57.43 °C), and T_8 (57.15 °C). The highest temperatures were consistently recorded at positions T_7 and T_8, situated in the central region of the drying chamber. At the same time, the lowest values were observed at position T_5, located near the peripheral zones.Throughout the experimental period, the system operated under variable meteorological conditions with a mean solar radiation intensity of 538.92 W/m². The complete thermal profile data, including minimum, maximum, and average temperature values for all monitoring points, are systematically presented in Table 1. The temporal evolution of temperature within the drying cabinet is illustrated in Figure 7, exhibiting characteristic response patterns that correspond to variations in solar input. Figure 9 provides a detailed representation of solar radiation fluctuations throughout the testing period, capturing the intermittent transitions between clear sky conditions (peak intensity: 875.00 W/m²) and cloud cover events (minimum intensity: 67.50 W/m²). This variability in solar radiation presented an opportune scenario for evaluating system resilience and performance stability under realistic operational conditions.

Table 1. Compare the temperature with the intensity of solar radiation.

Temp(°C)	**min**	**max**	**av**
T_1	36.88	64.92	50.33
T_2	39.10	63.05	48.67
T_3	31.18	39.92	34.92
T_4	36.83	60.63	50.22
T_5	37.25	58.34	47.27
T_6	42.43	68.29	54.31
T_7	43.57	71.58	57.43
T_8	39.80	70.47	57.15
I_o(W/m²)	67.50	875.00	538.92

Temperature measurement sensors were strategically distributed throughout the drying chamber to characterize the three-dimensional thermal profile, resulting in observable temperature gradients across the monitored volume (Figure 3). Spatial thermal analysis revealed a systematic temperature distribution pattern, with the highest temperature (57.43 °C) consistently recorded at sensor position T_7, located in the central region of the drying chamber. This central thermal maximum can be attributed to the convergence of convective currents and the cumulative radiative heat transfer from the surrounding copper pipe network. Conversely, the lowest operational temperature was documented at position T_1 (50.33 °C), situated at the inlet junction of the heat exchanger, where the introduction of the working fluid creates a localized cooling effect. This temperature differential of approximately 7.1 °C between the chamber's central and peripheral regions demonstrates the importance of thermal stratification considerations in drying system design and the need for optimized flow distribution to ensure uniform product drying conditions.

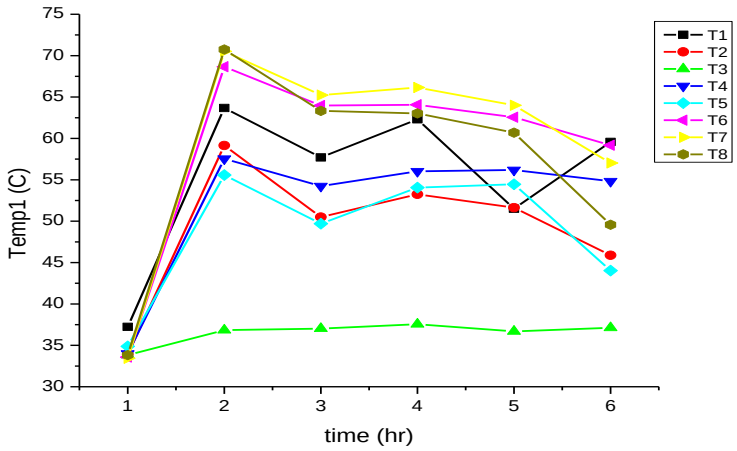

Figure7. The drying chamber's temperature

Comprehensive thermal performance data collected from the drying chamber are systematically compiled in Table 1, presenting minimum, maximum, and average temperature values for each measurement point over the experimental duration. The temporal evolution of these temperature profiles throughout the operational period (09:00-14:00) is graphically represented in Figure 7, illustrating the dynamic thermal response of the system under variable solar insolation conditions. This time interval was specifically selected to capture the maximum solar radiation availability period while documenting the system's thermal behavior during the transition from morning warming to midday peak conditions. The temperature curves demonstrate a characteristic rapid rise during the initial heating phase (09:00-10:00), followed by relative stabilization with fluctuations corresponding to ambient conditions and solar radiation intensity changes.

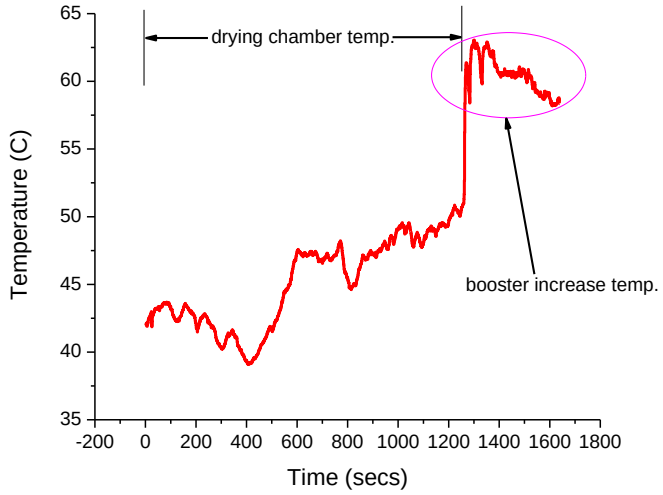

Figure8. The drying chamber's temperature, as well as the booster's increased temperature

The hybrid system demonstrated superior thermal response characteristics to conventional solar dryers, achieving rapid temperature elevation within the drying chamber in under five minutes. This accelerated heating rate can be attributed to the enhanced heat transfer mechanism facilitated by the pulsed copper pipe network, which efficiently conducts thermal energy from the hot water reservoir to the drying environment. Quantitative analysis of the temperature-time profile, as illustrated in Figure 8, revealed an initial heating rate of approximately 3°C per minute, enabling the system to reach operational temperature thresholds significantly faster than traditional passive solar dryers, which typically require 20-30 minutes to achieve comparable thermal conditions. This rapid thermal response represents a critical advancement for applications requiring prompt initiation of the drying process. It protects against transient solar radiation fluctuations by maintaining stable internal temperatures despite external environmental variations.

3.7. Environmental Conditions and Solar Resource Assessment

The experimental trials were conducted under variable meteorological conditions characterized by alternating clear sky and cloud cover periods. This weather pattern provided an opportune scenario for evaluating system performance across a spectrum of solar radiation intensities. Continuous monitoring via calibrated pyranometer recorded solar radiation fluctuations throughout the testing period, with values ranging from 67.50 W/m² during heavily clouded intervals to 875.00 W/m² during optimal clear sky conditions, yielding a mean radiation intensity of 538.92 W/m². These representative mixed-sky conditions are typical of the tropical climate at the experimental location and provide realistic operational parameters for assessing the system's resilience to radiation variability—a critical consideration for practical solar drying applications.

3.8. Dryer Efficiency Analysis

The thermal performance of the drying system was quantitatively evaluated using efficiency metrics that relate moisture removal capacity to solar energy input, as Equation (4) defines dryer efficiency as the ratio of heat energy effectively utilized for moisture evaporation to the total incident solar radiation on the collector surface. All efficiency calculations were performed using a constant aperture area (A_p) of 0.70 m² (0.7 m × 1.0 m) for analytical consistency.This efficiency parameter was calculated as:

$$\eta = \frac{\dot{m} \times h_{fg}}{A_p \times I_o} = \frac{26.53 \times 444.11}{07 \times 523.22} = 32.17\ \%$$

Where the mass flow rate of moisture removal (ṁ) was 26.53 kg/hr, the latent heat of vaporization (h_fg) was 444.11 kJ/kg, and the average solar radiation intensity (I_o) was measured at 523.22 W/m². The resulting efficiency value of 32.17% represents a significant improvement over conventional direct sun drying methods, which typically achieve 8-10% efficiencies under similar conditions.

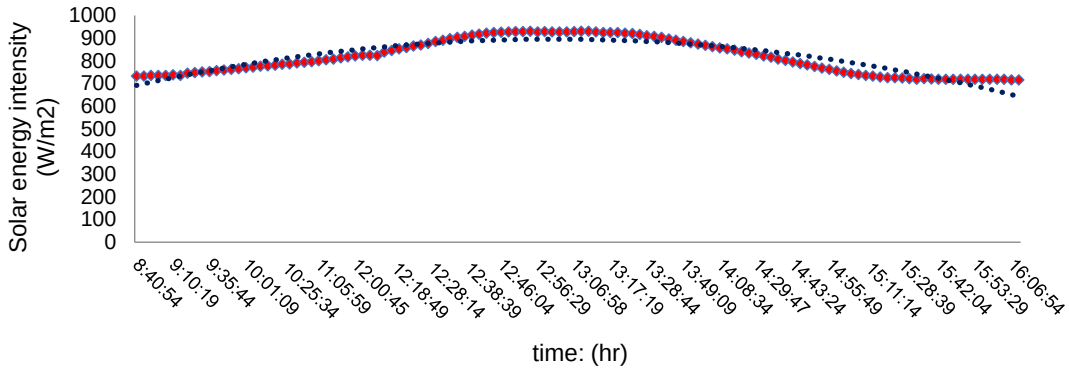

Figure 9. Solar radiation intensity

Table 2. The efficiency of the heat energy dryer, combined with hot water

Dryertype	T_{av}(°C)	$\dot{m}$ (kg/hr)	$I_{\circ}$ (W/m²)	h_{fg} (kJ/kg)	η (%)
DR	35.1	6.87	514.49	434..35	8.28
SR	46.20	8.45	523.22	435.46	10.05
SR+W50	45.10	26.53	523.22	444.11	32.17
SR+W50	47.08	26.55	531.58	446.18	31.83
SR+W50	49.43	19.61	348.73	449.21	36.08
SR+W60	51.30	15.47	552.64	450.67	18.02
SR+W60	52.16	25.94	538.92	451.53	31.12
SR+W60	54.53	22.55	496.35	453.92	29.46
SR+W70	63.67	16.51	841.29	463.13	12.98

Comparative analysis of the thermal performance data presented in Table 2 reveals significant efficiency variations among different operational configurations of the infrared combined heat and hot water dryer. The system demonstrated optimal performance at the intermediate temperature regime across the three controlled temperature setpoints (50 °C, 60 °C, and 70 °C). Specifically, the highest thermal efficiency of 36.08% was achieved when operating at an average chamber temperature of 49.43 °C, with corresponding process parameters including a moisture removal rate of 19.61 kg/s, average solar radiation intensity of 348.73 W/m², and latent heat of vaporization of 449.21 kJ/kg during the water phase transition. This peak efficiency point represents the optimal balance between thermal energy input and effective moisture removal capacity, as graphically illustrated in Figure 10. Notably, the efficiency-temperature relationship exhibits a non-linear response curve, with performance first increasing from 32.17% at 45.10 °C to the peak value of 36.08% at 49.43 °C, followed by a substantial decline to 12.98% at the highest temperature setpoint of 63.67 °C. This performance degradation at elevated temperatures can be attributed to increased thermal losses through the chamber walls and accelerated air circulation that reduces effective moisture extraction despite higher energy consumption. Identifying this optimal operational temperature range (approximately 48-52 °C) provides crucial guidance for maximizing energy utilization efficiency while maintaining effective drying capacity.

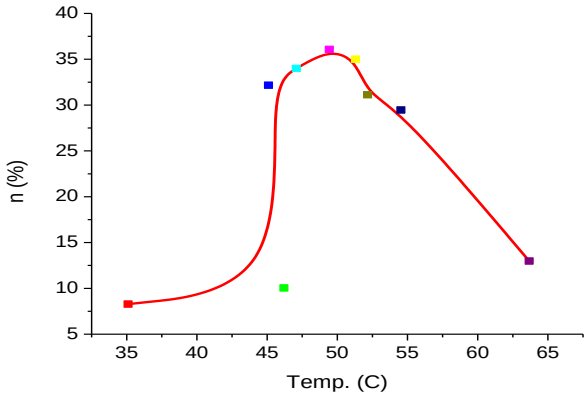

Figure 10. Efficiency of a dryer using infrared heat and hot water at a controlled temperature of 50, 60, and 70 °C

3.9 Comparative Performance of Drying Technologies

The combined infrared radiation and hot water heat dryer demonstrated exceptional thermal efficiency when operating within its optimal temperature range. At the ideal operating point, with an average chamber temperature of 49.43 °C, the system achieved a peak efficiency of 36.08%. This performance optimization occurred at the middle temperature setpoint within the experimental range (50 °C, 60 °C, and 70 °C), indicating that moderate temperature regimes provide the most favorable balance between energy input and moisture removal capacity.Comprehensive comparative analysis of the three distinct drying methodologies investigated in this study revealed substantial performance differentials:This traditional approach yielded the lowest thermal efficiency at 8.28%, reflecting substantial energy losses through uncontrolled radiation, convection, and lack of energy recovery mechanisms.The enclosed solar drying chamber showed modest improvement with an efficiency of 10.05%, representing a 21.4% increase over the direct drying method. This enhancement can be attributed to the contained environment that reduces convective losses and better directs solar radiation toward the product.The hybrid system incorporating pulsed copper pipes achieved a remarkable efficiency of 36.08%, representing a 335.7% improvement over traditional direct drying and a 259.0% enhancement compared to the conventional solar cabinet. This substantial performance gain derives from the system's ability to maintain optimal drying conditions through supplementary heating during periods of reduced solar radiation.

The superior performance of the integrated hybrid system extends beyond mere efficiency metrics. The advanced dryer design enables precise temperature control, improving product quality and consistency. Additionally, the system sustains the drying process for extended periods compared to conventional methods, allowing continuous operation even during unfavorable weather conditions or low solar insolation. This extended processing capability significantly enhances production capacity and reliability, as well as critical commercial or community-scale implementation factors.

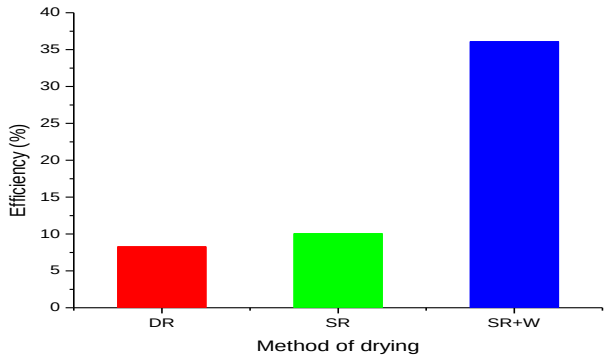

Figure 11. Compare the DR, SR, and SR+W dryers' performances.

4. Conclusions

This research demonstrates the successful development and validation of an innovative hybrid drying system that integrates infrared radiation with hot water circulation through pulsed copper pipes. The system employs a dual thermal energy approach: primary solar energy capture via flat-plate collectors for water heating, and subsidiary thermal energy transfer to the drying chamber through an engineered copper pipe network. This configuration creates a controlled thermal environment that effectively addresses the limitations of conventional solar drying methods. Experimental performance evaluation revealed exceptional thermal efficiency of 36.08% under optimized operating conditions, specifically at an average chamber temperature of 49.43 °C, with corresponding process parameters including a moisture removal rate of 19.61 kg/s, solar radiation intensity of 348.73 W/m², and latent heat of vaporization of 449.21 kJ/kg during the phase transition of water from liquid to vapor. This efficiency represents a substantial improvement over traditional drying approaches, with performance gains of 335.7% compared to direct sun drying and 259.0% relative to conventional solar cabinet drying. The hybrid system demonstrated remarkable thermal response characteristics, achieving operational temperature within two minutes of activation and sustaining stable thermal conditions for periods exceeding one hour. This rapid heating capability, combined with extended thermal persistence, addresses a critical challenge in solar drying applications: maintaining effective drying conditions during periods of reduced solar radiation, such as cloudy weather, evening hours, or monsoon seasons. Beyond efficiency metrics, the system offers significant practical advantages, including precise temperature control for optimized product quality, extended operational hours independent of immediate solar availability, and enhanced commercial or community-scale implementation reliability. The integration of pulsed copper pipes for heat conduction represents a cost-effective technological advancement that substantially improves the versatility and applicability of solar drying systems across diverse geographical and climatic conditions. Future research directions should explore optimization of pipe configuration for further efficiency improvements, investigation of thermal storage enhancements to extend operational duration, and comprehensive product quality assessment across various agricultural commodities to establish optimal drying parameters for specific applications.

5. Acknowledgements

We would like to thank Asst. Prof. Yuvalak Wetchawittayakun, President of Dhonburi Rajabhat University, for including permission to use the research venue.

Author Contributions: Author Contributions: The methodology strategy and techniques were conceptualised and designed by P.P, and K.K. It was P.P. and K.K. who implemented the construction, collected the data, analysed the results, and came to a conclusion. The authors P.P., and K.K. contributed to the writing and the general content modification.

Funding: Dhonburi Rajabhat University, which provided funding for this research.

Conflicts of Interest: The authors of this study hereby state that they have no conflicts of interest.

References

[1] Phoosomma, P. Construction and Efficiency Test of Solar Drying Cabinet for Nipa Palm Drying for Community Enterprise. In *Proceedings of the 18th International Conference on Control, Automation and Systems (ICCAS)*, PyeongChang, South Korea, 17-20 October 2018; pp. 1414-1417.

[2] Korbuakaew, K.; Phoosomma, P. Prototype a Food Processing Combination Heated Drying Cabinet. In *Proceedings of the 37th International Technical Conference on Circuits/Systems, Computers and Communications (ITC-CSCC)*, Phuket, Thailand, 4-7 July 2022; pp. 1-4. https://doi.org/10.1109/ITC-CSCC55581.2022.9894865

[3] Vengsungnle, P.; Jongpluempiti, J.; Srichat, A.; Wiriyasart, S.; Naphon, P. Thermal performance of the photovoltaic–ventilated mixed mode greenhouse solar dryer with automatic closed loop control for Ganoderma drying. *Case Stud. Therm. Eng.* **2020**, *21*, 100659. https://doi.org/10.1016/j.csite.2020.100659

[4] Nain, S.; Ahlawat, V.; Kajal, S.; Anuradha, P.; Sharma, A.; Singh, T. Performance analysis of different U-shaped heat exchangers in parabolic trough solar collector for air heating applications. *Case Stud. Therm. Eng.* **2021**, *25*, 100949. https://doi.org/10.1016/j.csite.2021.100949

[5] Amiri, S.; Gorji, B.; Bandpy, M.; Jahanshahi, M. Drying behaviour of lemon balm leaves in an indirect double-pass packed bed forced convection solar dryer system. *Case Stud. Therm. Eng.* **2018**, *12*, 677-686. https://doi.org/10.1016/j.csite.2018.08.007

[6] Fadhil, A.; Jalil, J.; Bilal, G. Experimental and numerical investigation of solar air collector with phase change material in column obstruction. *J. Energy Storage* **2024**, *79*, 110066. https://doi.org/10.1016/j.est.2023.110066

[7] Sharma, M.; Atheaya, D.; Kumar, A. Performance evaluation of indirect type domestic hybrid solar dryer for tomato drying: Thermal, embodied, economical and quality analysis. *Therm. Sci. Eng. Prog.* **2023**, *42*, 101882. https://doi.org/10.1016/j.tsep.2023.101882

[8] Chouicha, S.; Boubekri, A.; Mennouche, D.; Berrbeuh, M.H. Solar Drying of Sliced Potatoes an Experimental Investigation. *Energy Procedia* **2013**, *36*, 1276-1285. https://doi.org/10.1016/j.egypro.2013.07.144

[9] GaneshKumar, P.; Sundaram, P.; Sathishkumar, A.; Vigneswaran, V.S.; Chopra, T.; Thakur, U.; Kim, S.; Ramkumar, V. Exploring the performance of an indirect solar dryer by combining three augmentation approaches (trapezoidal absorber, shot blasting, and pebble stone). *J. Energy Storage* **2024**, *78*, 110109. https://doi.org/10.1016/j.est.2023.110109

[10] Murthy, M.V.R. A review of new technologies, models and experimental investigations of solar driers. *Renew. Sustain. Energy Rev.* **2009**, *13*, 835-844. https://doi.org/10.1016/j.rser.2008.02.010

[11] Gautam, A.; Chamoli, S.; Kumar, A.; Singh, S. A review on technical improvements, economic feasibility and world scenario of solar water heating system. *Renew. Sustain. Energy Rev.* **2017**, *68*, 541-562. https://doi.org/10.1016/j.rser.2016.09.104

[12] Bernardo, L.; Davidsson, H.; Karlsson, B. Retrofitting Domestic Hot Water Heaters for Solar Water Heating Systems in Single-Family Houses in a Cold Climate: A Theoretical Analysis. *Energies* **2012**, *5*, 4110-4131. https://doi.org/10.3390/en5104110

[13] Koua, K.; Fassinou, W.; Prosper Gbaha, P.; Siaka Toure, S. Mathematical modelling of the thin layer solar drying of banana, mango and cassava. *Energy* **2009**, *34*, 1594-1602. https://doi.org/10.1016/j.energy.2009.07.005

[14] Ismail, M.A.; Idriss, E.M.I. Mathematical modelling of thin layer solar drying of whole okra (Abelmoschus esculentus (L.) Moench) pods. *Int. Food Res. J.* **2013**, *20*, 1983-1989.

[15] Heydari, A. Experimental analysis of hybrid dryer combined with spiral solar air heater and auxiliary heating system: Energy, exergy and economic analysis. *Renew. Energy* **2022**, *198*, 1162-1175. https://doi.org/10.1016/j.renene.2022.08.110

[16] Yang, H.; Wang, J.; Wang, N.; Yang, F. Experimental study on a pulsating heat pipe heat exchanger for energy saving in air-conditioning system in summer. *Energy Build.* **2019**, *197*, 1-6. https://doi.org/10.1016/j.enbuild.2019.05.032

[17] Bastakoti, D.; Zhang, H.; Li, D.; Cai, W.; Li, F. An overview on the developing trend of pulsating heat pipe and its performance. *Appl. Therm. Eng.* **2018**, *141*, 305-332. https://doi.org/10.1016/j.applthermaleng.2018.05.121

[18] Barba, M.; Bruce, R.; Bouchet, F.; Bonelli, A.; Baudouy, B. Effects of filling ratio of a long cryogenic Pulsating Heat Pipe. *Appl. Therm. Eng.* **2023**, *194*, 117072. https://doi.org/10.1016/j.applthermaleng.2021.117072

[19] Nikolayev, V. Physical principles and state-of-the-art of modeling of the pulsating heat pipe: A review. *Appl. Therm. Eng.* **2021**, *195*, 117111. https://doi.org/10.1016/j.applthermaleng.2021.117111

[20] Li, Z.; Sarafraz, M.M.; Mazinani, A.; Moria, H.; Iskander Tlili, I.; Tawfeeq Alkanhal, T.; Goodarzi, M.; Safaei, M. Operation analysis, response and performance evaluation of a pulsating heat pipe for low temperature heat recovery. *Energy Convers. Manag.* **2020**, *222*, 113230. https://doi.org/10.1016/j.enconman.2020.113230

[21] Nazari, M.A.; Ahmadi, M.H.; Ghasempour, R.; Shafii, M.B.; Mahian, O.; Kalogirou, S.; Wongwises, S. A review on pulsating heat pipes: From solar to cryogenic applications. *Appl. Energy* **2018**, *222*, 475-484. https://doi.org/10.1016/j.apenergy.2018.04.020

[22] Nikolayev, V. Effect of tube heat conduction on the single branch pulsating heat pipe start-up. *Int. J. Heat Mass Transf.* **2016**, *95*, 477-487. https://doi.org/10.1016/j.ijheatmasstransfer.2015.12.016

[23] Jo, J.; Kim, J.; Kim, S. Experimental investigations of heat transfer mechanisms of a pulsating heat pipe. *Energy Convers. Manag.* **2019**, *181*, 331-341. https://doi.org/10.1016/j.enconman.2018.12.027

[24] Kumar, N.; Tripathi, M.M. Design of a Novel Solar Energy Market Model for Indian Scenario. *J. Electr. Eng. Technol.* **2021**, *16*, 2783–2792. https://doi.org/10.1007/s42835-021-00802-9

[25] Alsharif, M.; Yahya, K.; Geem, Z. Strategic Market Growth and Policy Recommendations for Sustainable Solar Energy Deployment in South Korea. *J. Electr. Eng. Technol.* **2020**, *15*, 803-815. https://doi.org/10.1007/s42835-019-00331-6

[26] Davidsson, H.; Bernardo, R.; Hellström, B. Hybrid Ventilation with Innovative Heat Recovery-A System Analysis. *Buildings* **2013**, *3*, 245-257. https://doi.org/10.3390/buildings3010245

[27] Mohamed, I.; Idriss, E.M. Mathematical modelling of thin layer solar drying of whole okra (Abelmoschus esculentus (L.) Moench) pods. *Int. Food Res. J.* **2013**, *20*, 1983-1989.

[28] Chouicha, S.; Boubekri, A.; Mennouche, D.; Berrbeuh, M. Solar Drying of Sliced Potatoes. An Experimental Investigation. *Energy Procedia* **2013**, *36*, 1276-1285. https://doi.org/10.1016/j.egypro.2013.07.144

[29] Nazari, M.; Ahmadi, M.; Ghasempour, R.; Shafii, M.; Mahian, O.; Kalogirou, S.; Wongwises, S. A review on pulsating heat pipes: From solar to cryogenic applications. *Appl. Energy* **2018**, *222*, 475-484. https://doi.org/10.1016/j.apenergy.2018.04.020